Available online at www.sciencedirect.com
SCIENCE DIRECT®
Journal of Power Sources 127 (2004) 331–340
JOURNAL OF POWER SOURCES
www.elsevier.com/locate/jpowsour

A new monitoring method for electrochemical aggregates by impedance spectroscopy

P. Kurzweil [a,*], H.-J. Fischle [b]

[a] *University of Applied Sciences, Kaiser-Wilhelm-Ring 23, D-92224 Amberg, Germany*
[b] *Hydra Supercap GmbH, Sickingenstraße 71, D-10553 Berlin, Germany*

Abstract

A variant of ac impedance spectroscopy is applied to monitor and control electrochemical cells and appliances without need for reference values and knowledge of control points in advance. Electrolyzers, fuels cells, energy stores, sensors and electrochemical reactors are steered to an optimum operating state by continuous evaluation of capacitance and the derivatives thereof. Dry and humid electrode–electrolyte interfaces are distinguished with the aid of the low-frequency impedance. The problem is solved in order to determine electrolyte concentrations unambiguously from electrolyte resistance, although the conductivity of the solution has a maximum and changes nonlinearly with the concentration.

Keywords: Derivative impedance spectroscopy; Capacitance; Electrolyte concentration; Water electrolysis; Supercapacitors; Metal oxide electrodes

1. Introduction

Electrolyzers for hydrogen and oxygen production, fuel cells, batteries, supercapacitors, solar cells, and electrochemical sensors form more or less sensible components of modern energy stores, propulsion systems and other technical aggregates [1–3]. Electrochemical devices open up promising applications. There have been trials to combine alkaline water electrolysis, solar modules and fuel cells in regenerative energy storage systems. Water electrolysis is well on the way to provide the oxygen supply for the astronauts in future space stations and in long-distance air-liners [4–7]. Electrolytically produced hydrogen offers to reduce harmful exhaust gases of internal combustion engines. All these applications require a self-regulating electrolyzer, which works reliably and safely without human manipulations.

Fuel cells for the mass markets must also be adapted to maintenance-free long-time operation. At best, in the laboratory scale all single cells of a stack might be monitored by help of a process guiding system. Future automotive systems require fuel cells, which are automatically controlled depending on the load demand. The driver of an electric car is not able to pay attention to single cell voltages, current, gas supply, water management and other critical parameters during a long-distance trip. Present fuel cells in test vehicles are damaged irreversibly during a highway race. There is urgent need for a method to pilot electrochemical aggregates through critical operating states.

For a hundred years, electric conductivity has been employed to characterize electrochemical cells. Recent patents [8] illustrate how the humidity of the solid polymer membrane in a fuel cell can be checked by means of the electrolyte resistance at a given frequency (1–20 kHz). A required amount of water is added until the membrane resistance reaches a given reference value nearby its minimum. Then the fuel cell is supposed to provide its maximum current. But there is no experimental certainty that the electrochemical system really works at its optimum operating point.

Our approach considers besides the electrolyte also the electrode reactions and the mass transport in the electrochemical device. The proposed method allows to monitor and control all the regular and critical operating states of the technical system. Reference values and control points are not required in advance. The impedance is measured again and again, and changes between current and preceding spectra are numerically determined by help of equivalent parallel capacitance [9], which is the real part of complex capacitance C. This is calculated from the frequency response of *ac* impedance $Z = \mathrm{Re}\,Z + i\,\mathrm{Im}\,Z$ or admittance $Y = 1/Z$ by Eq. (1).

$$C(\omega) = \mathrm{Re}\,C = \frac{\mathrm{Im}\,Y}{\omega} = \frac{-\mathrm{Im}\,Z}{\omega|Z|^2} = \frac{-\mathrm{Im}\,Z}{\omega[(\mathrm{Re}\,Z)^2 + (\mathrm{Im}\,Z)^2]} \quad (1)$$

* Corresponding author.
E-mail address: p.kurzweil@fh-amberg-weiden.de (P. Kurzweil).

0378-7753/$ – see front matter © 2003 Elsevier B.V. All rights reserved.
doi:10.1016/j.jpowsour.2003.09.030

Nomenclature

C	capacitance (in F)
C_{dl}	double layer capacitance (in F)
C_{el}	capacitance of electrolyte space or membrane
f	frequency (in Hz)
$R = \mathrm{Re}\ Z$	resistance, real part of impedance (in Ω)
R_{ct}	charge transfer resistance (in Ω)
R_{el}	electrolyte resistance (in Ω)
R_{oo}	resistance of cables and contacts
$X = \mathrm{Im}\ Z$	reactance, imaginary part of impedance (in Ω)
$Y = 1/Z$	admittance (in Ω^{-1})
$Z(\omega)$	impedance (in Ω)
Z_d	mass transport impedance (in Ω)
$\omega = 2\pi f$	circular frequency (in s^{-1})

It is not correct to write capacitance simply by $C = -(\omega\,\mathrm{Im}\,Z)^{-1}$, which would imply that the electrochemical cell behaves like a *RC*-series combination, whereby the polarization resistance is neglected. Eq. (1) fits for any equivalent circuit.

Nearby every electrochemical system shows an impedance spectrum in the complex plane which consists of three regions [9–11]. Simply speaking, every phase boundary causes its own arc in the complex plane. This is shown in the general equivalent circuit for most electrochemical systems in Fig. 1. Note the mathematical convention of impedance in the Figures, which show the negative imaginary parts on the negative imaginary axis.

1. The high frequency arc characterizes the electrolyte. In highly conducting solutions only the point of intersection with the real axis is visible and called the electrolyte resistance R_{el}.
2. The complex plane plot at medium frequencies reflects the electrode reactions, especially the charge transfer at the electrode–electrolyte interface.
3. The low-frequency arc mostly shows the influence of mass transport at the interface between electrode, electrolyte and gas phase and is described by a mass transport impedance Z_d. This can be modeled by a Nernst impedance (with finite thickness of diffusion layer), a Warburg impedance (with infinite diffusion layer) or a Randles equivalent circuit [10,11].

The electrolyte resistance is determined as the intersection point with the real axis in the complex plane according to Eq. (2). It may contain the resistance of cables R_{oo} (see Fig. 1).

$$R_{el} = \lim_{\omega\to\infty} \mathrm{Re}\ Z(\omega) \tag{2}$$

The capacitance approaches the value of the double layer capacitance at very high frequencies. If the electrolyte resistance is more or less exactly known, double layer capacitance is given by Eq. (3).

$$C_{dl} = \lim_{\omega\to\infty} \frac{-\mathrm{Im}\ Z}{\omega[(\mathrm{Re}\ Z - R_{el})^2 + (\mathrm{Im}\ Z)^2]} \tag{3}$$

Different from the impedance imaginary parts in the complex plane, capacitances include the frequency information and can be interpreted as a measure of electrode activity, surface coverage, and the state-of-charge of an energy store. Moreover, the separation of impedance in discrete regions

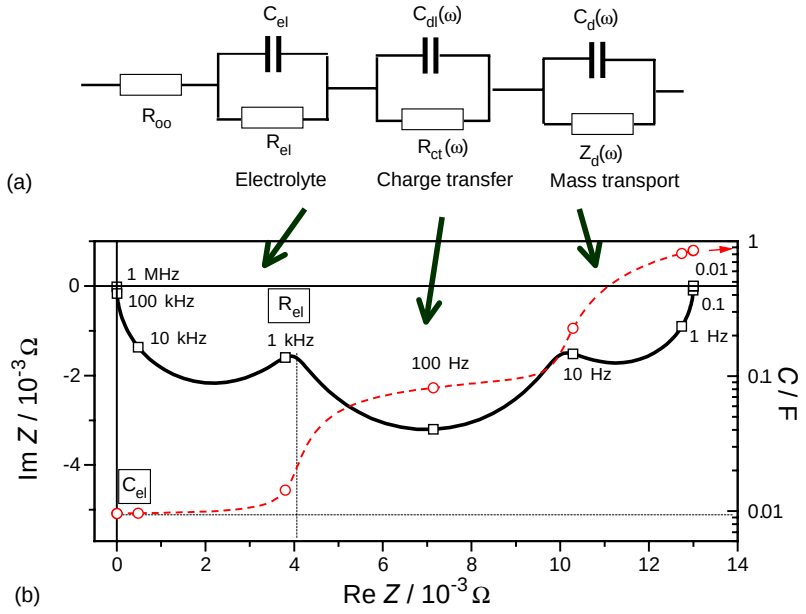

Fig. 1. General equivalent circuit of an electrochemical system (a) and simplified frequency response of impedance and capacitance (b). Note the mathematical convention of impedance.

allows us to determine whether the electrode–electrolyte interface is dry or humid. We use the electrolyte resistance as a measure for the electrolyte concentration and the water content of electrolyte spaces or solid polymer membranes respectively. Examples are illustrated in the following. The optimum operating state of the electrochemical system under test is reached at the highest capacitance and lowest resistance. To find out the optimum operating state a *C–R* plot is employed in the following as shown in Fig. 4. Imperceptible changes become obvious when the derivatives of capacitance and resistance are evaluated, a method which we call *derivative impedance spectroscopy* (DIS) [10].

2. Experimental

A Solartron 1250 frequency response analyzer was used to record the impedance spectra of various electrochemical devices under regular and critical operating conditions. Depending on whether the electrochemical system behaves as a current source or a current sink, a small ac current perturbation is modulated above the dc current of an electronic load or power source respectively which is connected to the electrochemical device. We call this the galvanostatic experiment. To a passive element or an electrochemical system at its open circuit potential, the frequency response analyzer can directly be connected. In the case that the electrochemical device is investigated under different voltages, a small ac voltage is modulated (potentiostatic experiment).

Instead of a frequency response analyzer, impedance measurements succeed using ac bridges, lock-in amplifiers or Fourier transform techniques. For technical applications in the mass markets, a low-cost circuitry working at two up to ten discrete frequencies is sufficient.

The novel principle of data analysis, which marks out the proposed monitoring method, is shown in the flow chart in Fig. 2. Focusing on the low-frequency arc, the graphical type of the impedance spectrum is determined. The linear region at low-frequencies is typical for a diffusion impedance or the so-called Warburg behavior and characterizes a humid electrode–electrolyte interface (type *A*), whereas a semicircular region (type *B*) gives a hint at a dry interface. The type of spectrum allows to determine whether the measured electrolyte resistance belongs to a dry or a wet operating state, and whether the related electrolyte concentration lies above or below the maximum of conductivity. In a second step, electrolyte resistance and capacitance are calculated according to the above Eqs. (1) and (2). The diagram of capacitance versus resistance depicts clearly the best operating point in the direction of the left edge above. When capacitance and resistance depart from this empirically given optimum, an output quantity such as current or water feed in the electrochemical device has to be changed.

3. Results and discussion

3.1. Water electrolysis

An electrolyzer with fixed alkaline electrolyte [5–7] consists of a series combination of bipolar single cells, each consisting of oxygen space, anode, electrolyte, cathode, hydrogen space and a metallic separator between the gas spaces of adjacent cells. The electrolyte, a concentrated potassium hydroxide solution, is fixed in the pores of an oxidic matrix

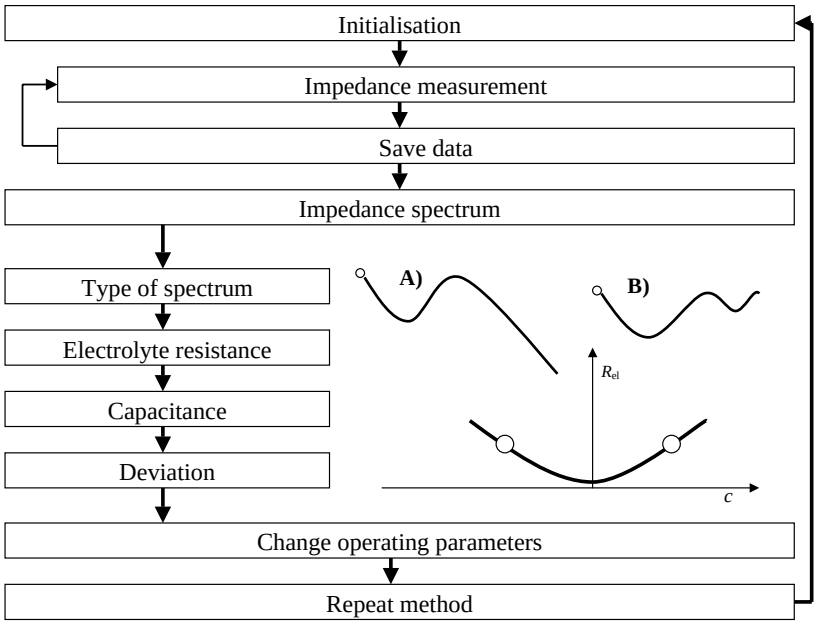

Fig. 2. Flow chart of the new monitoring method with analysis of the graphical type of the impedance spectrum and the chronological changes of capacitance and resistance.

material. The decisive problem for the long-time electrolysis is to control the water feed, so that the matrix never dries out and dangerous oxyhydrogen gas is never formed. On the other hand, the mass flow of water, which is provided to the electrolyte by permeation through a membrane, must not be too high. Otherwise, the electrolyte spaces and the porous electrodes are flooded and corrosive hydroxide solution penetrates into the gas spaces. Most difficult is the initial phase, when the electrolyzer is run to the final operating point and system pressure, whereby temperature and current are changed in short intervals of time. Moreover, during continuous electrolysis there are not any operating points durable for ever, as even slow fluctuations of temperature cause dramatical changes of water feed after a delay of some hours. The incessant demand of oxygen and hydrogen by astronauts or other users requires consecutive changes of current. There is need for a detailed insight into the electrolyzer, despite changing electrolyte concentrations and the inevitable degradation of the electrodes.

3.1.1. Diagnostic criteria for the water management

Fig. 3 illuminates the changes of impedance when the water content in the electrolyte spaces and porous electrodes passes from a dry operation state through the optimum to a wet state. This may happen within half an hour in the real system. The impedance in the complex plane consists of two arcs. The high-frequency arc *2* describes the rate-determining step of charge transfer. The point of intersection with the real axis marks the electrolyte resistance *1*. Dry and humid operation states can be separated by means of the low-frequency diffusion arc in the impedance spectrum. Two cases can be distinguished:

- At a wet electrode–electrolyte interface, the Warburg impedance *3* occurs, which is caused by a water film acting as diffusion barrier for the gas deposition. To avoid the danger of flooding the electrolyte spaces, the current has to be increased and the water feed to be reduced immediately.
- At a dry electrode–electrolyte interface a low-frequency circular arc *4* occurs. To avoid the danger that the electrolyte spaces dry out and oxyhydrogen gas forms, the current has to be reduced immediately.

The best operating state is given by spectrum *2*, as explained below.

3.1.2. Optimum operating state

Most evidently, the diagram of capacitance versus resistance (Fig. 4) shows regular and critical operation states during long-time electrolysis. The optimum operating state is reached at the highest capacitance and the lowest electrolyte resistance *2*. Then the electrode reactions are highly efficient, the waste heat is minimal and the water content of the electrolyte spaces is best. In real time operation, the electrolyzer swings slowly between a more dry and a more humid operation state. At continuous electrolysis, cell current and water feed are reduced or increased until the capacitance reaches its maximum. In the initial state of electrolysis, especially after a system breakdown or an extraordinary demand of oxygen, all operating parameters (pressure, temperature, current, etc.) are carefully changed in the one direction so that the capacitance climbs and the resistance falls. This principle, which does not require any operation points known in advance, is shown in Fig. 7. Vice versa, *whenever capacitance falls and resistance climbs, the electrochemical system runs into a critical state*. In the example in Fig. 7, an explosive oxyhydrogen mixture was formed within 3 h of electrolysis at 30 A and insufficient water feed. As the changes of capacitance and resistance are mostly small, the critical point at 5.5 h is detected too late in a post mortem analysis. Contrary to that, the method in Fig. 2 allows an

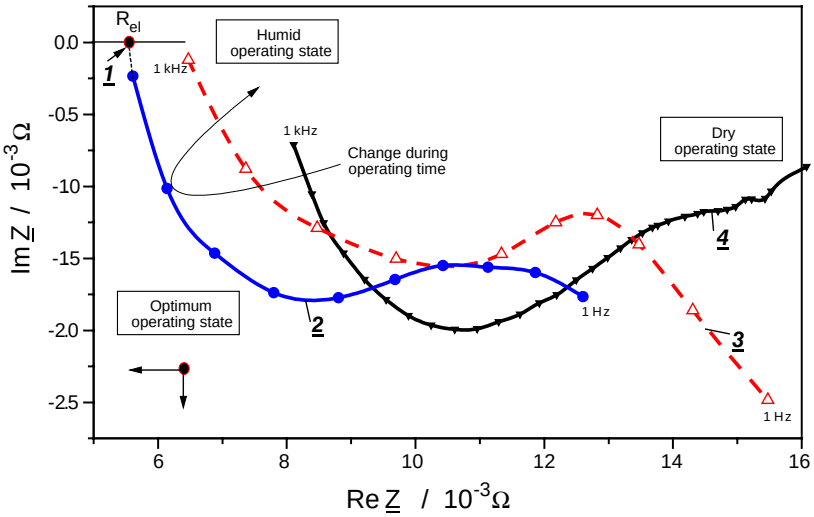

Fig. 3. Complex plane plots of impedance (mathematical convention) at an electrolyzer with fixed alkaline electrolyte, which show a humid and a dry electrode–electrolyte interface.

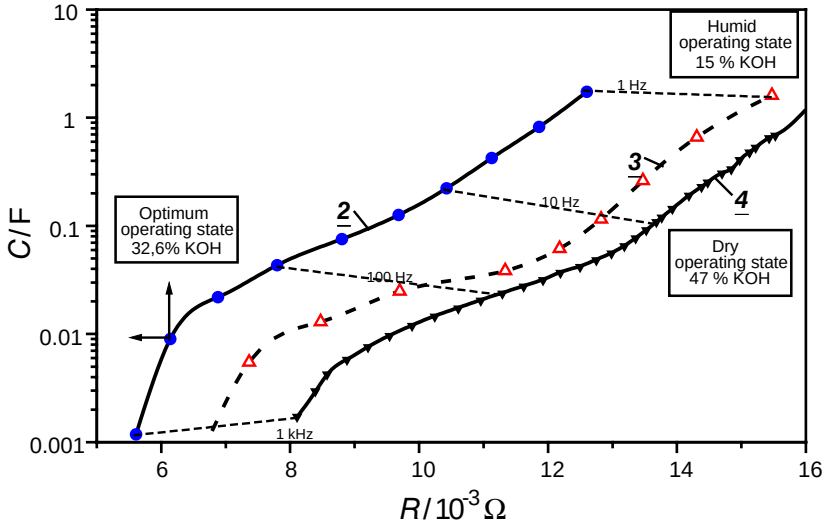

Fig. 4. Capacitance versus resistance during the long-time operation of an electrolyzer, which passes the optimum at the highest capacitance and the lowest electrolyte resistance.

online analysis and provides the best operating state at the lowest resistance and highest capacitance (at 2.5 h). Any deviation from this point during some minutes of operation at constant temperature and pressure signals that a current change is urgently necessary. With this monitoring method the electrolyzer swings around the optimum operating point, which is determined again and again, so that the optimum may change itself very slowly.

3.1.3. Analysis of critical operating states

The impedance spectrum gives hints at the effectiveness of the electrode reactions, the electrolyte concentration, mass transport, and surface coverage with absorbed hydrogen and oxygen. Changes of the capacitance in the $C(R)$-plot are quantified by differences $\Delta C(\omega)$ at fixed values of resistance or frequency. Advanced algorithms such as pattern recognition or fuzzy logic can be used for a trend analysis. In Fig. 5, capacitance and its first *1* and second derivative *2* with respect to frequency are shown. Derivative impedance spectroscopy emphasizes any chronological changes of capacitance and resistance in different time domains so that "hidden" polarizations can be detected earlier than in the complex plane.

3.1.4. Electrolyte concentration

Most aqueous solutions show a maximum of conductivity at a certain concentration, and to a certain electrolyte resistance belong two arbitrary concentrations. This is shown for

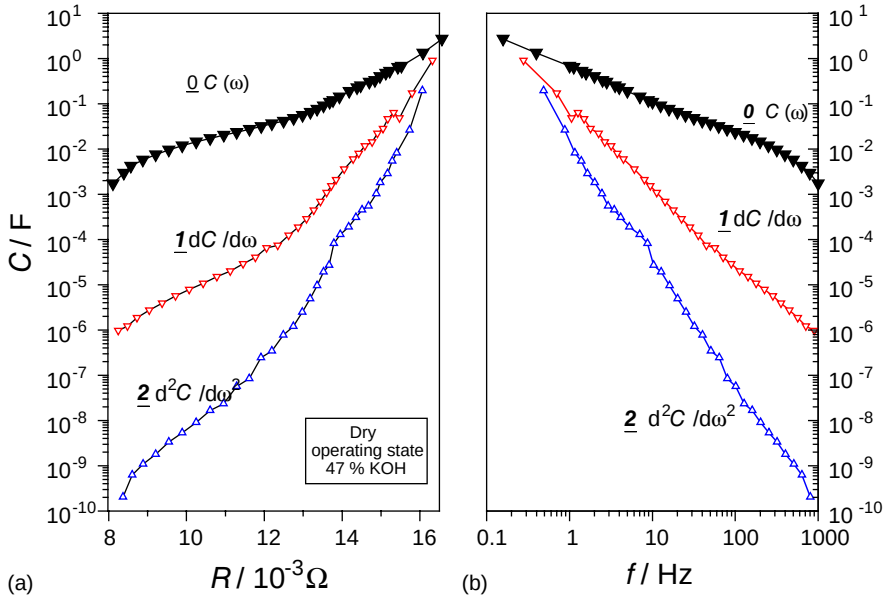

Fig. 5. Capacitance *0* and its first *1* and second derivative *2* with respect to frequency (b) and shown versus the real part of impedance (a).

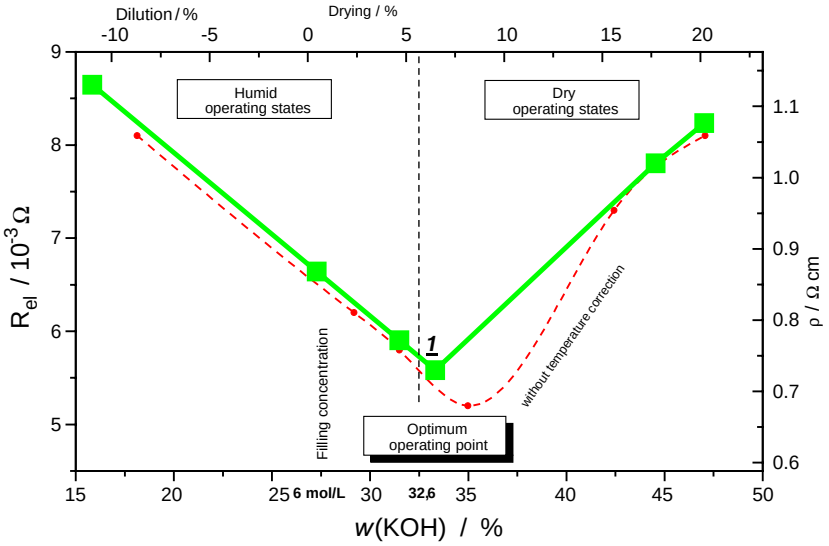

Fig. 6. The optimum operating point of an electrolyzer is situated at the electrolyte concentration (mass fraction) by which the electrolyte resistance reaches its minimum.

potassium hydroxide in Fig. 6. We solve the problem thanks to the low-frequency region *3* or *4* in Fig. 3, by determining whether the electrolyte resistance *1* measured belongs to a dry or a humid operating state. From literature [12], we know that the minimum electrolyte resistance R_{min} occurs in 32.6% KOH at 80 °C, which corresponds to the maximum of conductivity. In the following the ratio of resistances is considered, and the knowledge of the cell constant K or specific resistances are not required (but could be calculated if desired).

The change of water content in the electrolyte spaces is given by Eq. (4).

$$\chi = \frac{R - R_{min}}{R_{min}} \quad \text{and} \quad R_{min} = K \times 0.733\,\Omega\,\text{cm} \tag{4}$$

The mass fraction of potassium hydroxide in the solution with respect to the maximum of conductivity at 32.6% KOH reads:

$$\begin{aligned} w &= 32.6\% \times (1 - |\chi|) \quad \text{for} \quad \chi < 32.6\% \\ w &= 32.6\% \times (1 + |\chi|) \quad \text{for} \quad \chi > 32.6\% \end{aligned} \tag{5}$$

To calculate the molar concentration, the density ρ of the solution is required, which can be estimated as 1310 g/l. The molar mass M equals 56.11 g/mol.

$$c = \frac{\rho w}{M}(1 \pm |\chi|) \approx 7.6\,\text{mol/l}\,(1 \pm |\chi|) \tag{6}$$

Impedances measured at other temperatures than 80 °C (353 K) are corrected by use of an Arrhenius relation $\log R = A/T + B$. During the initial phase of electrolysis (see Fig. 7), the coefficients A and B are empirically determined using a least-squares fit line in a diagram of electrolyte resistance ($\log R$) versus $1/T$. Then Eq. (7) holds.

$$R_{80} = [R(T)]^C, \text{ wherein } C = \frac{A + B/353\,\text{K}}{A + B/T} \tag{7}$$

As the electrolyzer is automatically steered into the optimum operating state with the aid of capacitance, the filling concentration of the electrolyte and problems to calculate it play no longer any role. Finally, concentrations can be determined with the aid of the minimum electrolyte resistance given empirically during the initial state of long-time electrolysis (see Figs. 3 and 4). Thus, impedance spectroscopy qualifies for routine control of electrochemical cells, including the determination of electrolyte concentrations and the analysis of water management.

3.2. State-of-charge of a double-layer capacitor

As short-time energy stores with high power densities, so-called double-layer capacitors or supercapacitors have been described [13,14]. So far, the state-of-charge of capacitors, batteries and other energy stores has been determined by integrating the current versus time according to Eq. (8), which requires considerable effort. The measurement of capacitance provides the results in much shorter time by use of Eq. (1). Vice versa, Eq. (8) is useful to calculate electric charge after capacitance was measured at a low-frequency (where Q is electric charge, U the voltage, I the current, and t the time).

$$C = \frac{Q}{\Delta U} \text{ wherein } Q = \int I(t)\,\mathrm{d}t \tag{8}$$

The state-of-charge of the energy store is given by Eq. (9). As in a real supercapacitor capacitance depends on voltage, the state-of-charge does only approximately equal the ratio of the terminal voltages U/U_0.

$$\alpha = \frac{Q(U)}{Q(U_{max})} = \frac{C(U)}{C(U_{max})} \tag{9}$$

It is shown in Fig. 8 for a commercial supercapacitor how

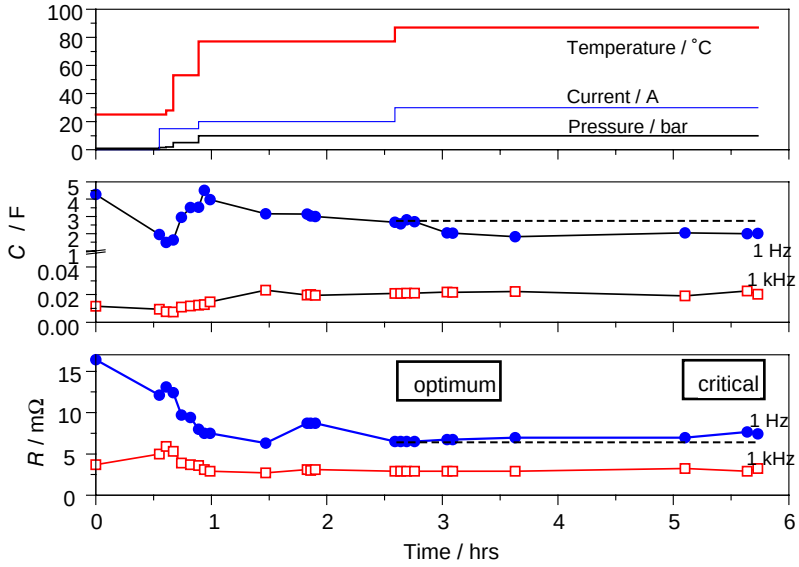

Fig. 7. Capacitance and resistance during the long-time operation of an electrolyzer, including the starting phase until the operating parameters reach their final values. Filled circles: low-frequency resistance and capacitance (1 Hz). Empty squares: high-frequency resistance and capacitance (1 kHz).

the state-of-charge influences the frequency response of capacitance. Both capacitance and stored energy depend on voltage. For the voltages applied, electric charge calculated by integration of current with respect to time ranges between 7.8 A (at 0.75 V) and 35.9 A (at 2.5 V), and strongly depends on the leakage current which has to be corrected. The capacitances calculated using Eq. (8) equal 10.3, 11.5, 11.7, and 13.4 F respectively, whereby the error due to the correction of the leakage currents equals up to 7%. The impedance measurement delivers directly the capacitances 10.5, 11.4, 11.7, and 12.1 F, and the state-of-charge values 87, 94, 97, and 100%., whithout need for determining leakage currents and other mathematical efforts. The error of routine impedance measurements equals approximately 1%. Thus, impedance spectroscopy qualifies for routine measurements of capacity and state-of-charge of double-layer capacitors and similar energy stores.

The diagram of capacitance versus resistance (Fig. 8) presents the performance data of a capacitor more clearly than the complex plane or Bode plot. Capacitance according to Eq. (8) changes its sign at a certain high frequency near the electrolyte resistance from positive (capacitive behavior) to negative (inductive behavior, for example in spiral wound devices). So, electrolyte resistance or equivalent se-

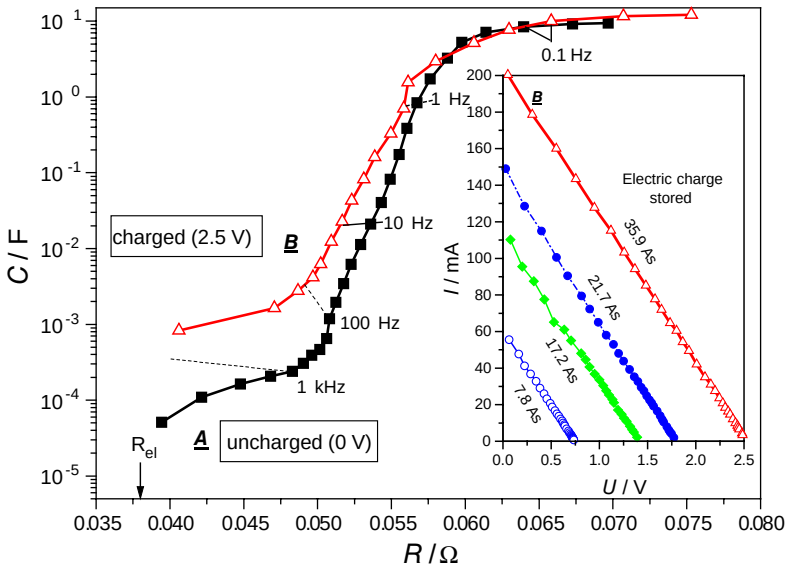

Fig. 8. Capacitance reflects the state-of-charge of a supercapacitor (10 F) at different voltages far more simply and quickly than by integrating current vs. time ($C = Q/U$). Small picture: current and electric charge at different charging voltages. *A* uncharged, *B* charged at 2.5 V.

ries resistance (ESR), minimum and maximum capacitance, and the transition to inductive behavior at high frequencies are obvious in a single diagram. The frequency response of capacitance reflects among other things the amount of surface area accessible to the electrolyte. Capacitance at high frequencies shows the "outer" electrode surface, which may depend on grain boundaries and other interparticle phenomena. Capacitance at low-frequencies shows the "inner" electrode surface, which is primarily determined by the pore size distribution and the speed of ion transport through the porous electrode (details are shown in [11,13–15]). This way, the measurement of capacitance and analysis of the *C–R* diagram supports the characterization of new materials and the monitoring of supercapacitors in practical applications. Again, the chronological changes of capacitance and resistance are investigated in order to determine whether for example a hybrid system of fuel cell and capacitor works at its optimum at high capacitance and low resistance (see 3.4). Vice versa, slowly decreasing capacitance and increasing resistance show the deterioration and estimated life time of the system.

3.3. Deterioration of technical electrodes

The proposed method is excellently qualified to judge the aging and useful life of electrodes. Technical electrosynthesis requires long-time stable electrocatalysts such as platinum metal oxides [16] for alkali chloride electrolysis, and lead dioxide [17] for ozone production. Lead dioxide coated on titanium supports and so-called DSA electrodes deteriorate during electrolysis at high current densities; this is due to the growth of a poorly conducting interlayer between electrocatalyst and support material. In the course of continuous electrolysis, a second arc forms at highest frequencies in the complex plane.

In Fig. 9, three electrodes show roughly the same impedance spectrum at high frequencies. At first sight, the diagram of capacitance versus resistance reveals that the electrode A1 with the highest capacitance is most active; A2 shows a lower activity (capacitance), and the electrode *B* with the highest resistance is not useful at high current densities due to the interlayer resistance of about 0.25 Ω, which causes an enormous waste heat.

Some capacitance and resistance values gathered at a fixed frequency during a long-time experiment are sufficient to extrapolate the useful life of the electrode. The change of resistance $\Delta R/R$ reflects the growth of the interlayer, the change of capacitance $\Delta C/C$ the decline of electrochemical activity.

3.4. Control of fuel cells

The proposed method works with fuel cells just in the same way as described for electrolysis. All ambient and system parameters are changed carefully in the one direction that the capacitance never declines, especially after unexpected events or temporary peak power operation. Beyond this recipe, the type of impedance spectrum gives valuable hints at water management, gas supply and mass transport.

3.4.1. PEM fuel cells

The qualitative impedance at low-temperature polymer electrolyte fuel cells has been intensively studied [18–20]. In the complex plane, the high-frequency arc above 1 kHz describes the PEM membrane. The electrolyte resistance depends on the membrane thickness *d* and reciprocal

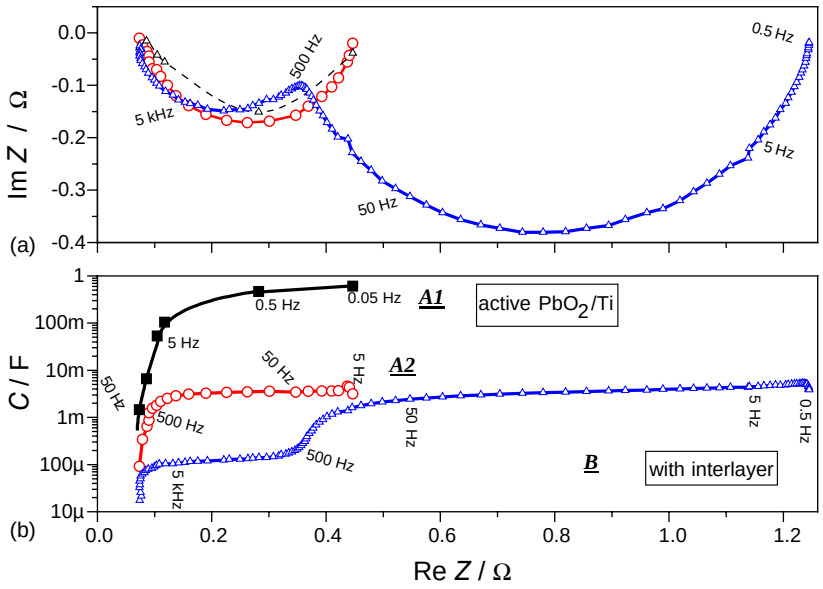

Fig. 9. Capacitance versus resistance (b) reveals more clearly than the complex plane plot (a) the performance of titanium electrodes coated with lead dioxide during long-time electrolysis in 0.5 molar sulfuric acid solution at high current densities (A1 highly active, A2 less active, *B* unuseful electrode).

temperature $1/T$, but not on current. The water content of the membrane can be estimated analogous to Section 3.1.4.

The geometric capacitance as a measure for the effective interface area between membrane and electrode can be estimated by the electrolyte resistance and the frequency f_m at the minimum of the membrane arc in the complex plane according to Eq. (10) or can be extrapolated from capacitance versus resistance or frequency (see Fig. 1).

$$C_{el} = \frac{R_{el}}{2\pi f_m} \tag{10}$$

The arc at medium frequencies describes the activity of the electrocatalyst (charge transfer process). As the hydrogen electrode works as a quasi reference electrode, the impedance is determined by the cathodic oxygen reduction. The better the electrocatalyst for the oxygen reduction the smaller is the second arc.

The low-frequency section of the impedance spectrum shows the limiting mass transport which is connected with the rate-determining electrode reaction, especially the diffusion of reactant gases and product water. At a wet interface between membrane, electrode and gas phase, the above mentioned diffusion impedance occurs, because a thin water film hinders the access of hydrogen and oxygen to the electrocatalyst. At a dry interface, a low-frequency semicircle appears. The problems of flooding and drying out are the same as described above for the electrolysis. The optimum operating state shows a maximum capacitance and a low resistance.

3.4.2. Solid oxide fuel cells

The high-frequency semicircle in the complex plane in Fig. 10 describes the solid oxide [11,21], typically zirconium oxide stabilized with yttrium oxide. At medium frequencies, the electrode reaction (charge transfer) is observed. The low-frequency semicircle reveals the gas supply. The C–R plot in Fig. 10 shows a good operating state *1* at high capacitance and low resistance. A disadvantageous change of system parameters, such as a insufficient hydrogen supply, brings about the "bad" curve *3*. Thus, impedance spectroscopy qualifies for monitoring all types of fuel cells without great effort.

3.5. Detecting chemical substances

The proposed method can be applied to electrochemical sensors. Capacitance reflects the dielectric properties of ionic conducting layers [22,23]. Water absorbed or produced by a chemical reaction changes the resistance, and capacitance shows the adsorption and desorption of the target molecules on the electrode surface.

Fig. 11 shows the frequency response of impedance and capacitance of a zeolite-based interdigital capacitor, which was tested as a sensor for butane gas. At the platinum catalyst in the zeolite layer, hydrocarbons are converted into carbon dioxide and water. The plot of capacitance versus resistance or frequency proves that 250 °C is the best operating temperature, and that the absorption and conversion of butane deteriorates both the resistive and the capacitive properties of the sensor. The measuring frequency for the detection of the hydrocarbon conversion should lie below 50 Hz. Product water can be observed above 1 kHz, and shows a slight increase of capacitance and conductivity. Thus, impedance spectroscopy qualifies as a simple monitoring method even for electrochemical sensors.

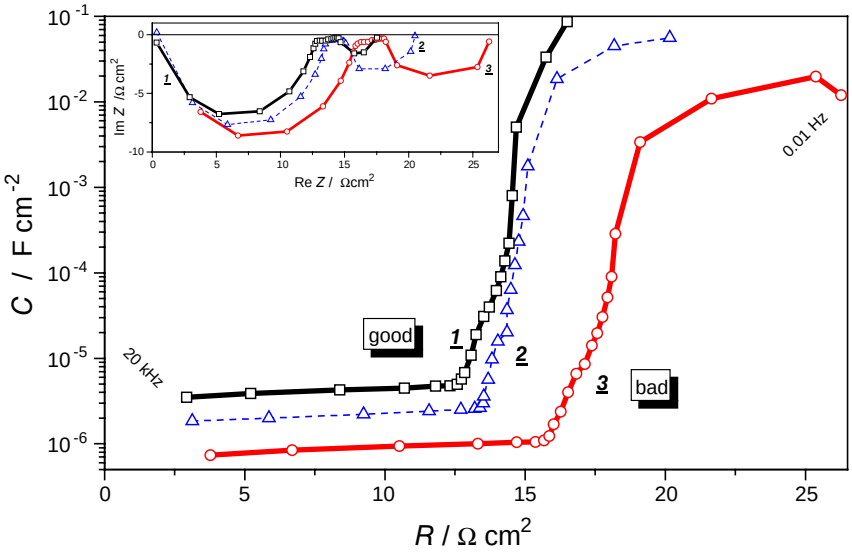

Fig. 10. Regular and critical operating states of a solid oxide fuel cell (20 cells, 17 V, 1000 °C) appear more clearly in the capacitance plot versus resistance than in the complex plane (small picture). Different water content of the fuel gas hydrogen (curve *2* → *3* at 300 mA/cm^2) and change of current (curve *1*: 100 mA/cm^2; *2*: 300 mA/cm^2).

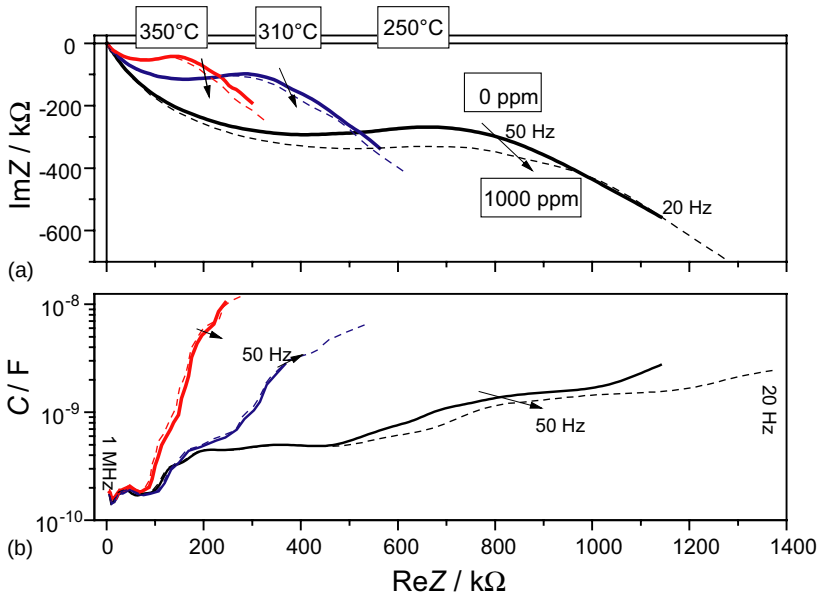

Fig. 11. Complex plane plots (a) and frequency response of capacitance versus resistance (b) of an electrochemical sensor [22] at different temperatures in air and 1000 ppm butane (dashed line).

4. Conclusion

The proposed monitoring method has proved to be a simple method to control various electrochemical devices. The optimum operating point is found by help of a *C–R* diagram at the highest possible capacitance and the lowest resistance. Dry and wet electrode–electrolyte interfaces are distinguished by means of the low-frequency semicircular or linear impedance respectively. With this, electrolyte concentrations can be directly determined from electrolyte resistances, whereby the minimum value is empirically determined during the initial operating phase of the device (when capacitance reaches its maximum). Furthermore, the frequency response of capacitance and impedance describe water management, gas supply and other parameters influencing the performance of electrochemical aggregates.

References

[1] J. Garche (Ed.), Angewandte Elektrochemie, in: Proceedings of the 1st Ulm Electrochemical Talks, Universitätsverlag Ulm, 1994.
[2] C.H. Hamann, W. Vielstich, Elektrochemie, Wiley–VCH, Weinheim, 1998.
[3] L.J.M.J. Blomen, M.N. Mugerwa (Eds.), Fuel Cell Systems, Plenum Press, New York, 1993.
[4] R.J. Davenport, J. Power Sources 36 (1991) 235–250.
[5] U. Benz, H. Preiss, O. Schmid, Dornier Post, No. 2, 1992.
[6] H. Funke, G. Tan, SAE Technical Paper Series No. 961371 Presented at 26th International Conference on Environmental Systems, Monterey, CA, 8–11 July 1996.
[7] P. Kurzweil, O. Schmid, European Patent EP 0 764 727 B1, 1999.
[8] A. Koschany, C. Lucas, Th. Schwesinger, German Patent DE 196 48 995 C 2, 2001.
[9] P. Kurzweil, German Patent Application DE 102 20 172, 2002.
[10] P. Kurzweil, IDA Computer Program for Impedance Data Analysis, Kyrill & Method, Verlag, München, 1991.
[11] J. R. Macdonald, Impedance Spectroscopy, Wiley, New York, 1987.
[12] Landolt-Börnstein, Numerical Data and Functional Relationships in Science and Technology, Springer, Berlin.
[13] S. Trasatti, P. Kurzweil, Platinum Met. Rev. 38 (1994) 46–56.
[14] P. Kurzweil, H.-J. Fischle, in: Proceedings of the 11th International Seminar on Double Layer Capacitors, Deerfield Beach, USA, 3–5 December 2001.
[15] W. Schmickler (Ed.), Ladungsspeicherung in der Doppelschicht, in: Proceedings of the 2nd Ulm Electrochemical Talks, Universitätsverlag Ulm, 1995, pp. 291–310, and literature cited therein.
[16] S. Trasatti, Electrodes of Conductive Metallic Oxides, Part A, Elsevier, Amsterdam, 1980.
[17] D.W. Wabner, H.P. Fritz, D. Missol, R. Huss, F. Hindelang, Z. Naturforsch. 31b (1976) 39–44, 45–50.
[18] I. Rubinstein, J. Rishpon, S. Gottesfeld, J. Electrochem. Soc. 133 (1986) 729–734.
[19] A. Parthasarathy, B. Davé, S. Srinivasan, A.J. Appleby, C.R. Martin, J. Electrochem. Soc. 139 (1992) 1634–1641.
[20] T.E. Springer, T.A. Zawodzinski, M.S. Wilson, S. Gottesfeld, J. Electrochem. Soc. 143 (1996) 587–599.
[21] P. Kurzweil, Technical report, Dornier GmbH, Friedrichshafen, 1993.
[22] P. Kurzweil, W. Maunz, C. Plog, Sens. Actuators, B 24–25 (1995) 653–656.
[23] C. Plog, W. Maunz, P. Kurzweil, E. Obermeier, C. Scheibe, Sens. Actuators, B 24–25 (1995) 403–406.